

Bio-optical relationships and ocean color algorithms for the north polar region of the Atlantic

Malgorzata Stramska

Hancock Institute for Marine Studies, University of Southern California, Los Angeles, California, USA

Dariusz Stramski

Scripps Institution of Oceanography, University of California, San Diego, La Jolla, California, USA

Ryszard Hapter, Slawomir Kaczmarek, and Joanna Stoń

Institute of Oceanology, Polish Academy of Sciences, Sopot, Poland

Received 30 October 2001; revised 30 October 2001; accepted 11 February 2003; published 13 May 2003.

[1] Up to now, relatively few bio-optical measurements have been made in the high northern latitude waters, which allow sound relationships for ocean color remote sensing to be determined. We collected optical and chlorophyll *a* concentration, *Chl*, data in the north polar region of the Atlantic in summer season. The investigated region includes subarctic and arctic waters between 70°N and 80°N within the meridional zone between 1°E and 20°E. Our measurements show that the current NASA global algorithms, OC2, OC4, and chlor-MODIS, generally overpredict *Chl* in the investigated waters by a factor of about 2 at low pigment concentrations (<0.2 mg m⁻³) and underpredict *Chl* at higher concentrations (20–50% at 2–3 mg m⁻³). For our data set, the best two-band algorithm for *Chl* involves the ratio of remote-sensing reflectance, $R_{rs}(442)/R_{rs}(555)$, at 442-nm and 555-nm light wavebands. We found that the general trend of variation in the blue-to-green reflectance ratio, $R_{rs}(442)/R_{rs}(555)$ or $R_{rs}(490)/R_{rs}(555)$, with *Chl* was driven primarily by *Chl*-dependent change in the green-to-blue ratio of absorption by pure seawater and particles. The effect of the blue-to-green backscattering ratio was of secondary importance. We observed a characteristic optical differentiation of waters within the investigated region. The majority of waters, which are here hypothesized to be dominated by diatoms, exhibited a relatively high blue-to-green reflectance ratio. The waters at several other stations, presumably dominated by dinoflagellates and/or prymnesiophytes, showed much lower reflectance ratio. Our data also show that the seemingly random variations in particulate absorption and backscattering coefficients at any given *Chl* are significant (more than a factor of 2) in the investigated waters.

INDEX TERMS: 4552 Oceanography: Physical: Ocean optics; 4275 Oceanography: General: Remote sensing and electromagnetic processes (0689); 9325 Information Related to Geographic Region: Atlantic Ocean; 9315 Information Related to Geographic Region: Arctic region; *KEYWORDS:* ocean optical properties, bio-optical algorithms, ocean color remote sensing, north polar Atlantic

Citation: Stramska, M., D. Stramski, R. Hapter, S. Kaczmarek, and J. Stoń, Bio-optical relationships and ocean color algorithms for the north polar region of the Atlantic, *J. Geophys. Res.*, 108(C5), 3143, doi:10.1029/2001JC001195, 2003.

1. Introduction

[2] Recent development of satellite ocean color sensors such as MODIS and SeaWiFS has been accompanied by an increased effort to establish algorithms for determining ocean optical properties, phytoplankton pigments, and primary production from ocean color imagery [Esaias *et al.*, 1998; Hooker and McClain, 2000]. It is generally known that the performance of ocean color algorithms can be better if algorithms and their parameters are established and applied on a regional basis, compared to the performance of a universal algorithm with a single set of parameters applied

indiscriminately to the entire global ocean. To this end, several studies proposed the partitioning of the world's oceans into provinces based on physical, chemical, biological, and/or bio-optical criteria [Platt and Sathyendranath, 1988; Mueller and Lange, 1989; Longhurst *et al.*, 1995; Esaias *et al.*, 2000; Hooker *et al.*, 2000]. One important advantage of regional approaches stems from the fact that bio-optical variability in a given region may be described and understood with significant accuracy if an appropriate database from in situ measurements exists for that region.

[3] Regional comparisons revealed significant differences between bio-optical data and algorithms from polar waters and lower latitudes [Mitchell and Holm-Hansen, 1991; Mitchell, 1992; Fenton *et al.*, 1994; Dierssen and Smith,

2000; *Sathyendranath et al.*, 2001]. However, insufficient optical measurements have been made in the high northern latitude waters to allow sound predictive relationships for remote sensing applications to be determined. The data from the Barents Sea and Fram Strait suggest differences in bio-optical relationships between these polar waters and temperate waters [*Mitchell*, 1992]. Similarly, the data from the Labrador Sea differ markedly from the chlorophyll-based ocean color model that was developed with low- and mid-latitude data [*Sathyendranath et al.*, 2001].

[4] The main goal of this study is to establish empirical relationships for estimating chlorophyll *a* concentrations and absorption coefficients from observations of remote-sensing reflectance in the north polar region of the Atlantic, which includes subarctic and arctic waters between 70°N and 80°N within the meridional zone between 1°E and 20°E. We will here describe the variability of the two inherent optical properties (IOPs) of seawater, i.e., the spectral absorption and backscattering coefficients, $a(\lambda)$ and $b_b(\lambda)$, which control the variability of spectral remote-sensing reflectance, $R_{rs}(\lambda)$. By analyzing the relation between the IOPs and the chlorophyll *a* concentration, *Chl*, we will provide insight into the variations of ocean color with *Chl* in the investigated waters. Based on our in situ data, we will also derive simple two-band ratio algorithms for retrieving chlorophyll concentration and absorption coefficient from observations of ocean reflectance. We will compare these algorithms with current NASA global algorithms that are based on much larger data sets but collected predominantly in low- and mid-latitude waters.

2. Conceptual Background

[5] Although the approaches based on the coupled atmosphere-ocean system are now emerging in the field of ocean color applications [e.g., *Yan et al.*, 2002], the present-day satellite ocean color algorithms usually involve two main separate steps of data processing. In the first step, which is commonly referred to as atmospheric correction, the effects of the atmosphere and sea surface are removed from satellite measurement of upwelling radiance [*Gordon and Wang*, 1994; *Gordon*, 1997]. In the second step, the empirical or semianalytical in-water algorithms are used to derive bio-optical properties of the ocean (such as chlorophyll concentration, diffuse attenuation coefficient of downwelling irradiance, or absorption coefficient) from water-leaving radiance or remote-sensing reflectance [e.g., *O'Reilly et al.*, 1998; *Carder et al.*, 1999].

[6] The semianalytical algorithms are typically based on an approximate relationship between the remote-sensing reflectance and the inherent optical properties (IOPs) of seawater,

$$R_{rs}(\lambda) \sim b_b(\lambda)/a(\lambda), \quad (1)$$

where the remote-sensing reflectance $R_{rs}(\lambda)$ is the ratio of the water-leaving radiance measured in the nadir direction just above the sea surface to downwelling plane irradiance incident on the sea surface, $a(\lambda)$ and $b_b(\lambda)$ are the absorption and backscattering coefficients of seawater respectively, and λ is the light wavelength in vacuum.

The $a(\lambda)$ and $b_b(\lambda)$ coefficients are the IOPs, which can be partitioned into additive components [e.g., *Mobley*, 1994],

$$\begin{aligned} a(\lambda) &= a_w(\lambda) + a_p(\lambda) + a_{CDOM}(\lambda), \\ a_p(\lambda) &= a_{ph}(\lambda) + a_d(\lambda), \\ b_b(\lambda) &= b_{bw}(\lambda) + b_{bp}(\lambda), \end{aligned} \quad (2)$$

where the subscripts w, p, ph, d, and CDOM denote pure seawater, total particulate assemblage suspended in water, phytoplankton, detrital particles (nonliving organic and mineral particles, and heterotrophic organisms), and colored dissolved organic matter, respectively. The underlying concept of semianalytical models is that if we can describe each component of backscattering b_b and absorption a , then we can determine the magnitude of these components from measurements of R_{rs} , given some assumptions about the angular distribution of light in the water [e.g., *Gordon et al.*, 1988; *Carder et al.*, 1991; *Lee et al.*, 1994; *Carder et al.*, 1999]. However, the natural bio-optical variability creates difficulties in quantifying some parameters of semianalytical models and at present such models usually do not provide better estimates of chlorophyll *a* concentration than simple empirical algorithms [*O'Reilly et al.*, 1998].

[7] In the empirical approaches, in situ measurements are usually used to relate the ratio of spectral remote-sensing reflectance, $R_{rs}(\lambda)$ (or normalized water-leaving radiance, $L_{wn}(\lambda)$ [see *Gordon*, 1997]), to the ocean parameters of interest such as the chlorophyll *a* concentration, *Chl*. The basis for the development of empirical algorithms has been the observation that changes in *Chl* in Case 1 waters [*Morel and Prieur*, 1977] are accompanied by more or less systematic variations in the ocean optical properties including the spectrum of ocean reflectance [*Gordon and Morel*, 1983; *Morel*, 1988]. As an example, the current NASA OC2 algorithm (Ocean Chlorophyll two-band algorithm) estimates *Chl* from a statistical relationship between *Chl* and the ratio $R_{rs}(490)/R_{rs}(555)$ described by a modified cubic polynomial formulation (i.e., a third-order polynomial plus an extra coefficient). The NASA OC4 algorithm estimates *Chl* from a fourth-order polynomial (five coefficients) by using the maximum band ratio determined as the greater of the $R_{rs}(443)/R_{rs}(555)$, $R_{rs}(490)/R_{rs}(555)$, or $R_{rs}(510)/R_{rs}(555)$ values [*O'Reilly et al.*, 2000]. The OC2 and OC4 (version 4) algorithms are presently used for routine global processing of SeaWiFS imagery. These algorithms are based on the largest data set (>2800 in situ observations) ever assembled for this type of algorithm development [*O'Reilly et al.*, 2000]. This data set includes, however, a relatively small number of data (about 10% of all observations) from only a few locations within the high northern latitude waters (Bering Sea, Labrador Sea, Resolute Bay).

[8] There also exist other two-band empirical algorithms; for example most pigment estimates from CZCS imagery involved the use of $L_{wn}(443)/L_{wn}(550)$ and $L_{wn}(520)/L_{wn}(550)$ ratios (see *O'Reilly et al.* [1998] for review of *Chl* algorithms). The current processing of MODIS Terra and Aqua imagery at NASA produces several pigment products, one of which, referred to as chlor_MODIS (MODIS Terra/Aqua Product 19 Parameter 14), is based on Clark's empirical relationship between *Chl* and the three-band ratio,

$[L_{\text{wn}}(442) + L_{\text{wn}}(487)]/L_{\text{wn}}(547)$. The bio-optical data used for developing this algorithm were collected only in low-latitude waters on the original NIMBUS-7 CZCS and the MODIS Marine Optical Characterization Experiment cruises for algorithm development (D. K. Clark, personal communication, 2002).

[9] In accordance with equation (1), the reflectance ratio is approximately equal to the product of backscattering ratio and absorption ratio,

$$R_{\text{rs}}(\lambda_1)/R_{\text{rs}}(\lambda_2) = [b_b(\lambda_1)/b_b(\lambda_2)][a(\lambda_2)/a(\lambda_1)]. \quad (3)$$

This equation provides a theoretical framework for the analysis of chlorophyll two-band algorithms, which are based on the variation of $R_{\text{rs}}(\lambda_1)/R_{\text{rs}}(\lambda_2)$ with *Chl*. As shown, this variation is driven by the changes in the spectral ratios of the two IOPs, $b_b(\lambda_1)/b_b(\lambda_2)$ and $a(\lambda_2)/a(\lambda_1)$, with *Chl*. Therefore, by measuring b_b and a (in addition to R_{rs} and *Chl*), one can develop an understanding of the empirical relationship between *Chl* and $R_{\text{rs}}(\lambda_1)/R_{\text{rs}}(\lambda_2)$. Specifically, the knowledge of b_b and a offers the opportunity to explain how these IOPs affect the general trend line as well as the spread of data in the relationship *Chl* versus $R_{\text{rs}}(\lambda_1)/R_{\text{rs}}(\lambda_2)$. A significant part of the present work is focused on such analysis.

3. Field Campaigns and Measurements

[10] Optical and chlorophyll data were collected in June–August of 1998, 1999, and 2000 during three cruises on the R/V *Oceania* operated by the Institute of Oceanology, Polish Academy of Sciences. Our field work was part of oceanographic research that has been conducted by this institute in the Arctic since 1987 [Piechura and Walczowski, 1995]. The study area extended between Norway and Spitsbergen, from about 70°N to 80°N within the meridional zone between 1°E and 20°E (Figure 1). This area represents the north polar region of the Atlantic, which includes waters of the Norwegian Sea, the confluence zone of the Norwegian Sea and Barents Sea, the West Spitsbergen Current, and the Greenland Sea. Some stations were visited on two or three cruises in different years and some stations were visited only on one cruise. At some stations all our in situ optical measurements and analyses of discrete water samples were accomplished, and at other stations only part of these measurements were made because of occasional technical problems with in situ instrumentation. In this study we analyze data from stations where we observed no evidence of significant influence of terrestrial materials on the optical properties of seawater. Therefore, a number of stations visited during the cruises, especially those located in fjords and coastal waters of western Spitsbergen where terrestrial input was significant (not shown in Figure 1), were excluded from this study.

3.1. In Situ Optical Profiles

[11] Optical measurements were made within the photic zone down to about 100–200 m in close proximity (time and space) to water samples collected with the Niskin bottles. We used a freefall spectroradiometer, SeaWiFS Profiling Multichannel Radiometer SPMR (Satlantic, Inc.), to measure vertical profiles of the downwelling irradiance

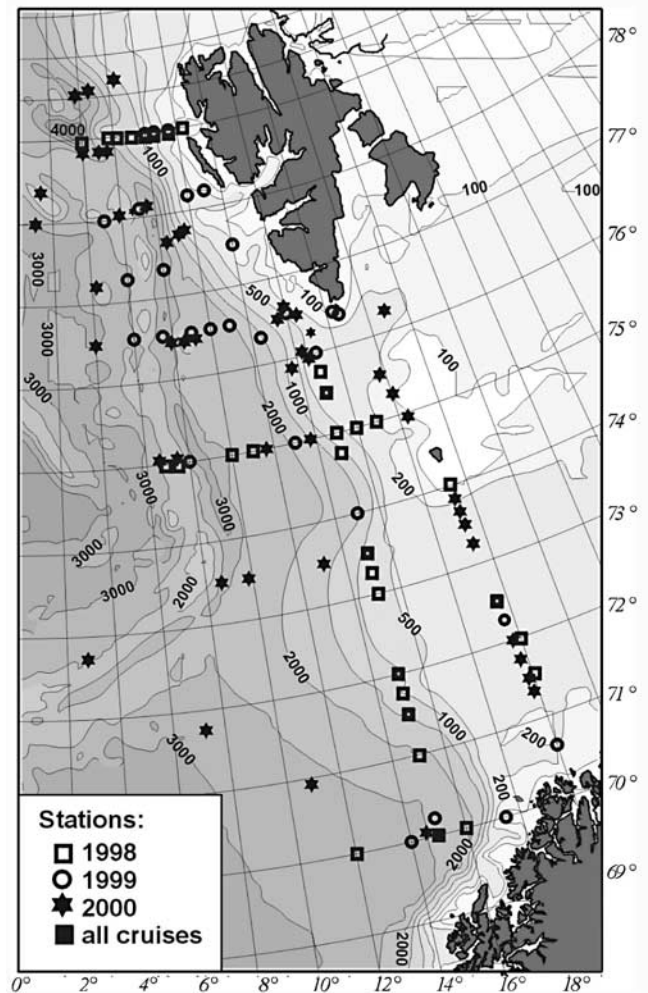


Figure 1. Map of the study region showing location of stations where optical measurements were made.

(E_d) and upwelling radiance (L_u) at 13 spectral wavebands (339, 380, 412, 442, 470, 490, 510, 532, 555, 590, 620, 666, and 682 nm) away from ship perturbations. The instrument was calibrated before each cruise, and data were processed with Prosoft software provided by Satlantic, Inc. The data were binned into 1-m depth intervals, and the vertical attenuation coefficients for downwelling irradiance (K_d) and upwelling radiance (K_l) were usually estimated using 10 bins. Profiles were visually inspected for quality, and a depth range within the upper mixed layer was selected for extrapolation of radiometric quantities to immediately beneath the sea surface. These radiometric measurements and data processing were consistent with methods described by Mueller and Austin [1995].

[12] We also used a multisensor datalogger system designed for measurement of the vertical profiles of the physical and optical properties of seawater. This system included a SeaBird Sealogger 25 with temperature, conductivity, and pressure sensors, a Hydroscat-6 backscattering sensor (HobiLabs, Inc.), two c-Star beam transmissometers (WetLabs, Inc.), a WetStar chlorophyll fluorometer (WetLabs, Inc.), and a PAR sensor (Biospherical Instruments, Inc.). The transmissometers provided measurements of the beam attenuation coefficient at 488 and 660 nm. The

Hydroscat-6 measured the volume scattering function at six wavebands (442, 470, 555, 589, 620, and 671 nm) at a fixed scattering angle centered at about 140°. On the cruise in 1998 the 510-nm waveband was used instead of the 555-nm band. The methodology of this measurement, calibration procedures, and subsequent determination of the backscattering coefficient are described by *Maffione and Dana* [1997]. To obtain the final estimates of $b_b(\lambda)$, the measurements were processed using Hydrosoft 2.06 software (HobiLabs, Inc.) with a standard built-in correction for the beam attenuation effect. We verified that the use of the beam attenuation measurements with the two c-Star transmissometers instead of the standard correction generally yielded $b_b(\lambda)$ values higher by a few percent (8% in the extreme case) but the blue-to-green b_b ratios were essentially the same (to within 2%). We chose to use the standard attenuation correction for all Hydroscat-6 measurements because the c-Star transmissometer data were occasionally unavailable. We also note that processing of our Hydroscat-6 measurements with Hydrosoft 2.06 yielded $b_b(\lambda)$ values lower by as much as 30% for the clearest waters encountered in the investigated region ($b_b(442) \approx 0.002 \text{ m}^{-1}$ and $Chl < 0.2 \text{ mg m}^{-3}$) compared to what would be obtained with previous versions of Hydrosoft software. This difference decreased with a decrease in water clarity. The blue-to-green b_b ratios obtained with Hydrosoft 2.06 were smaller by a few percent to 10% compared to earlier versions of data processing. Our final $b_b(\lambda)$ values at Hydroscat-6 wavebands were used to fit a power function, $b_b(\lambda) \sim \lambda^{-\gamma}$, which describes the spectral shape of $b_b(\lambda)$. The $b_b(\lambda)$ values at spectral bands matching the SPMR spectroradiometer bands were then obtained from this function.

3.2. Analysis of Water Samples

[13] At each station a sample of surface water was collected with a bucket. At most stations, samples were also collected at a few additional depths, typically within the surface mixed layer, using 10-L Niskin bottles. The time difference between the collection of water samples and acquisition of in situ optical data was less than half an hour. Because our interest is focused on bio-optical relationships relevant to remote sensing of ocean color, in this paper we use data from the analyses of surface water only. We note that the top 15–20 m (or deeper) layer was nearly homogeneous in terms of the measured IOPs at all stations included in the analysis.

3.2.1. Particulate Absorption

[14] The spectral absorption coefficients of particulate matter, $a_p(\lambda)$, were measured on freshly collected samples using a filter-pad technique [*Yentsch, 1962; Mitchell et al., 2000*]. The measurements were made with a dual-beam UV4-100 spectrophotometer (Unicam, Ltd) equipped with a 63.5-mm internal diameter Spectralon integrating sphere (RSA-UC-40 model, Labsphere, Inc.). Particles were collected by filtration under low vacuum onto 25-mm Whatman GF/F filters. The sample filters were placed at the transmittance sample port of the integrating sphere and scanned in the spectral range 350–750 nm. The optical density (absorbance) values at all wavelengths of the sample filters were corrected for the blank filter and background signal at 750 nm. Thus we made an assumption that

absorption by particles declines to zero at 750 nm [*Babin and Stramski, 2002*].

[15] The spectral absorption coefficients, $a_p(\lambda)$, were calculated from the corrected optical density of the sample filters, $OD_f(\lambda)$, using the equation

$$a_p(\lambda) = [2.303 OD_f(\lambda)A](V\beta)^{-1}, \quad (4)$$

where V is the volume of filtered seawater, A is the clearance area of the filter determined by measuring the diameter of the portion of the filter covered by the collected particles, and β is the path length amplification factor, which quantifies an increase of path length caused by scattering of light within the GF/F filter. Note that the V/A ratio is the geometric path length uncorrected for β , and $(\beta V)/A$ is the actual path length increased due to light scattering within the filter. The prevalent current practice to calculate $a_p(\lambda)$ for natural seawater samples involves the path length correction formulas reported in the literature, which are based mostly on β determinations for phytoplankton cultures [e.g., *Bricaud and Stramski, 1990; Mitchell, 1990; Cleveland and Weidemann, 1993*]. In this study we use our own β correction formulas determined from special experiments performed on our cruises with natural assemblages of marine particles. We made seven such β experiments, one on the 1998 cruise, three in 1999, and three in 2000. The experiments were made at stations that were selected to represent two general subregions of the study area, the transect from Norway to Spitsbergen and the area west of Spitsbergen.

[16] In the β experiments, we prepared samples of concentrated seawater. We used these samples to measure spectra of optical density of particles in suspension in 1-cm cuvette and spectra of optical density of particles collected on the GF/F filter. In both types of measurement, the optical densities were corrected for the appropriate blank and 750-nm background signals. To prepare the concentrated samples, seawater was filtered onto 0.2 μm Nuclepore filters and the collected particles were resuspended in a small volume of water. Typically, the final volume of the concentrated sample was several tens of milliliters and the required concentration of particles within such samples was obtained by filtering >10 L of seawater. In each β experiment, the concentrated sample was optically thin enough to ensure negligible multiple scattering of light within the 1-cm cuvette. Thus the measurements in the cuvette provided optical densities for 1-cm path length, that is with no effect of β (in other words, $\beta = 1$ for measurements on suspensions in 1-cm cuvette). In each experiment, the filter pad measurements were made on multiple filtration volumes of the concentrated sample to achieve a significant range of optical density on the GF/F filter, from less than 0.01 to about 0.4.

[17] In each β experiment we used data from the spectral range 400–700 nm to determine the relationship between the optical density of particle suspension with no β effect, OD_s , and the optical density of particles collected on the filter, OD_f , which is affected by the β factor ($\beta > 1$ for the measurements on GF/F filters). In the OD_s versus OD_f relationship, the OD_s values are derived by scaling optical densities measured on particle suspension over 1-cm path length to the geometric path length V/A used in the GF/F filter measurements. After such scaling, the ratio OD_f to

OD_s yields β . In agreement with previous experiments with phytoplankton cultures, a quadratic function of the form

$$OD_s = C_1 OD_f + C_2 OD_f^2 \quad (5)$$

generally provided a good fit to our OD_s versus OD_f data. C_1 and C_2 are coefficients of the least squares regression fit. The nonlinearity of this relationship indicates that β changes as a function of OD_f according to

$$\beta = (C_1 + C_2 OD_f)^{-1}. \quad (6)$$

We note that equation (6) shows no explicit dependence of β and OD_f on light wavelength λ because this relationship was obtained by pooling together the OD_s and OD_f data from the spectral region 400–700 nm. Equation (6) was used to calculate the β values needed in our routine determinations of $a_p(\lambda)$ from equation (4). For example, the coefficients $C_1 = 0.33$ and $C_2 = 0.983$ were obtained in the β experiment made at one station (74°N, 13°E) from the Norway-Spitsbergen transect in 1999. This correction was applied in the determination of $a_p(\lambda)$ for all stations occupied in this subregion in 1999. As another example, $C_1 = 0.557$ and $C_2 = 0.178$ were obtained from β experiments made at two stations (77°15'N, 6°E and 77°30'N, 12°E) in the area west of Spitsbergen in 1999. This correction was applied in the determination of $a_p(\lambda)$ for all stations occupied in the area west of Spitsbergen in 1999. Similar β corrections were applied for data collected in 1998 and 2000. We also note that in the second example above, β varies between about 1.8 and 1.6 for OD_f between 0.01 and 0.3, which represents the lowest β values among all our β experiments. In all other experiments, the β values were always greater than 2 for $OD_f < 0.17$, and mostly somewhat greater than the β estimates of Mitchell [1990].

[18] Immediately upon completion of the spectral scan for determining $a_p(\lambda)$, the sample GF/F filters were subject to a chemical treatment with NaClO for about 2 min. This technique bleaches the more labile pigments on the filter associated primarily with phytoplankton, leaving behind refractory absorbing material associated primarily with detritus [Tassan and Ferrari, 1995]. The treated filter was scanned again in the spectrophotometer to determine the spectral absorption coefficient of detritus, $a_d(\lambda)$. The phytoplankton absorption, $a_{ph}(\lambda)$, was then calculated as a difference between $a_p(\lambda)$ and $a_d(\lambda)$.

3.2.2. Pigments

[19] Pigments contained within suspended particles were collected by filtration of water samples onto 47-mm Whatman glass-fiber filters (GF/F) under low vacuum and extracted 24 hours in 96% ethanol at room temperature. Chlorophyll *a* concentration was determined spectrophotometrically with a UV4-100 spectrophotometer (Unicam, Ltd). The optical density of the extract at 665 nm was corrected for the background absorbance in the near infrared (750 nm), and converted to chlorophyll *a* concentration, *Chl*, using an equation involving the volumes of filtered seawater and ethanol extract, a 2-cm path length of cuvette, and the *Chl a*-specific absorption coefficient in 96% ethanol ($=83 \text{ dm}^3(\text{cm g})^{-1}$ [see Sch6tz, 1962; Marker et al., 1980, Nusch, 1980]).

[20] Additional samples were taken on the cruise in 1999 for analysis of pigments by high-performance liquid

chromatography (HPLC) and fluorometry. These samples were stored in liquid nitrogen until post-cruise analysis in the laboratory. For these samples the chlorophyll *a* concentration ranged from about 0.14 to 3.7 mg m^{-3} . *Chl* (*Chl a*) derived from the HPLC method [Goericke and Repeta, 1993] was calculated as the sum of chlorophyll *a* and derivatives (chlorophyllide *a*, chlorophyll *a* allomers and epimers). Fluorometric chlorophyll *a* was determined in 90% acetone extracts with a Turner Designs model 10-005 fluorometer following the standard procedure [Parsons et al., 1984; Trees et al., 2000]. Spectrophotometric and HPLC estimates of *Chl* were highly correlated and showed good agreement (on average to within 13.5%) with no systematic deviation between the two estimates. The linear regression analysis yielded the relationship

$$Chl(\text{spectrophotometric}) = 1.0239 Chl(\text{HPLC}) + 0.0123, \quad (7)$$

with the squared correlation coefficient $r^2 = 0.95$ and the number of observations $n = 50$. There is no significant difference between the estimated slope parameter and 1, as the standard error of the slope estimate is 0.0339. The difference between the intercept and 0 is also insignificant with the standard error of 0.0461 for the intercept estimate. All the *Chl* data used in the present paper represent the spectrophotometric values, which is supported by the comparison with HPLC-determined *Chl*. The fluorometric and HPLC-derived *Chl* values were also strongly correlated, but the fluorometric estimates showed a tendency to assume somewhat higher values than *Chl* derived from HPLC. The regression analysis yielded the relationship $Chl(\text{fluorometric}) = 1.1763 Chl(\text{HPLC}) - 0.0338$ ($r^2 = 0.968$, $n = 50$).

4. Results

4.1. Comparison of in Situ and Satellite-Derived Data

[21] We compared the normalized water-leaving radiances (L_{wn}) and chlorophyll *a* concentrations (*Chl*) estimated from our ship-based measurements and high resolution (HRTP) SeaWiFS data (Table 1 and Figure 2). L_{wn} is approximately the radiance that would exit the ocean in the absence of atmosphere with the Sun at the zenith [Gordon, 1997]. Following the criteria described by McClain et al. [1998] we excluded from this comparison the SeaWiFS data with land, cloud/ice, sun glint, and atmospheric correction failure, as well as the negative L_{wn} data. The time difference between the SeaWiFS and in situ observations was less than 2 hours and 4 hours for radiometric and chlorophyll comparisons, respectively. In situ radiometric and chlorophyll data were collected within 2 hours and 3 hours from the local solar noon, respectively. Because of overcast skies during the cruise in 2000, the data in Table 1 and Figure 2 include the results only from 1998 and 1999.

[22] The data presented in Table 1 indicate a large difference between in situ and satellite-derived water-leaving radiances (L_{wn}) in the blue spectral region. The $L_{wn}(490)/L_{wn}(555)$ ratio (or equivalently the $R_{rs}(490)/R_{rs}(555)$ ratio) shows, however, a fairly good agreement between in situ and satellite-derived values (see also Figure 2a). These ratios are thus less sensitive to possible errors in the atmospheric correction than the magnitude of L_{wn} (or R_{rs})

Table 1. Comparison of the In Situ and SeaWiFS Match-up Data

Parameter	Mean Ratio SeaWiFS/In Situ	Number of Observations
L_{wn} (412)	0.54	13
L_{wn} (443)	0.74	13
L_{wn} (490)	0.91	13
L_{wn} (510)	0.90	13
L_{wn} (555)	0.86	13
L_{wn} (490)/ L_{wn} (555)	1.06	13
Chl (in situ $0.2 < Chl < 0.45 \text{ mg m}^{-3}$)	1.623	12
Chl (in situ $0.9 < Chl < 1.67 \text{ mg m}^{-3}$)	0.764	9

at a single waveband. As a result, the observed errors in the SeaWiFS-derived chlorophyll a concentration from the OC2(version 4) algorithm (Table 1 and Figure 2b), can be primarily attributed to the performance of the OC2 algorithm itself. This comparison suggests that OC2 overestimates Chl for relatively low pigment concentrations, $Chl < 0.5 \text{ mg m}^{-3}$, and underestimates Chl for higher pigment concentrations ($>1 \text{ mg m}^{-3}$) in the waters investigated.

4.2. Chlorophyll Algorithms

[23] Figure 3 compares our in situ determinations of Chl with the estimates of Chl obtained from the in situ radio-

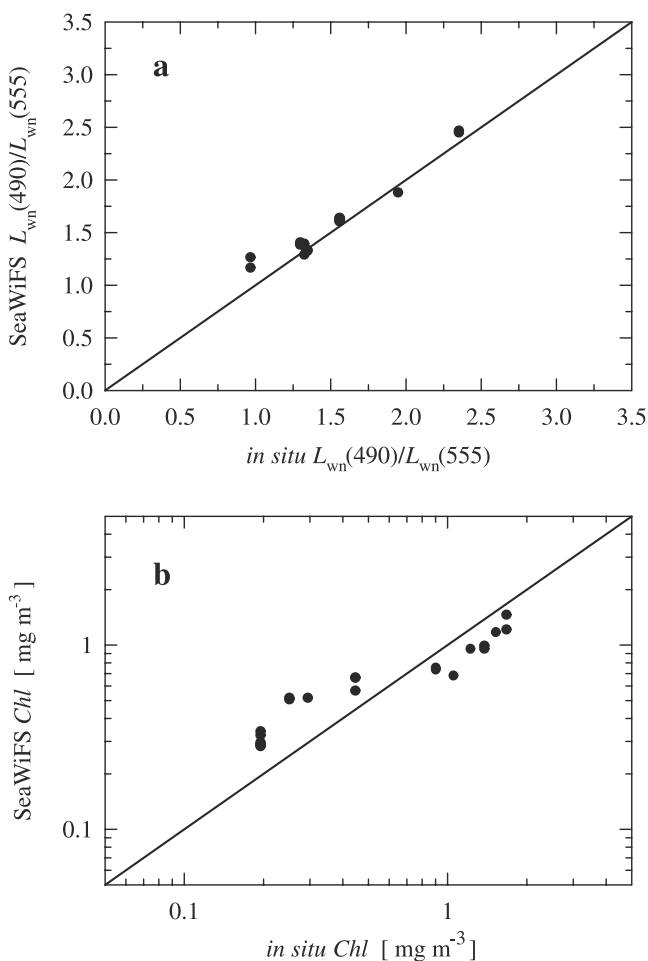


Figure 2. (a) Comparison of in situ and SeaWiFS-derived spectral ratio of normalized water-leaving radiance, L_{wn} . (b) Comparison of in situ and SeaWiFS-derived concentration of chlorophyll a , Chl .

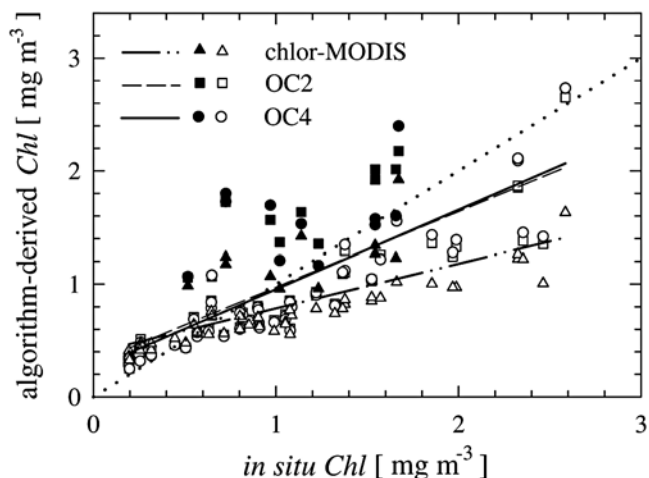


Figure 3. Comparison of chlorophyll a concentration from in situ determinations with chlorophyll a estimates derived from the three algorithms, chlor-MODIS (Clark’s algorithm for MODIS Terra/Aqua Product 19 Parameter 14), OC2 (version 4), and OC4 (version 4 [see O’Reilly *et al.*, 2000]). These algorithms were applied to our in situ spectroradiometric measurements. For each algorithm, the data points (open and solid symbols) and the best fit regression line are shown. The open symbols represent the usual stations, and the solid symbols represent the unusual stations (see text for details). Dotted line represents $y = x$.

metric measurements of R_{rs} and L_{wn} using the three algorithms, OC2, OC4, and chlor-MODIS. Although the data points show a relatively large scatter, the potential bias of these algorithms is evident. The OC2- and OC4-derived Chl values are generally similar. On average, these two algorithms overestimate Chl by a factor of about 2 at low Chl ($\approx 0.2 \text{ mg m}^{-3}$) and underestimate Chl by 20% when Chl is about 2.5 mg m^{-3} . The MODIS algorithm shows a more pronounced underestimation at high Chl (nearly a factor of 2 at $Chl 2.5 \text{ mg m}^{-3}$). These results are consistent with previous observations of systematic underestimation of Chl at intermediate to high pigment concentrations if bio-optical models based on low- and mid-latitude data are applied to the high northern latitude waters [Cota, 2001; Sathyendranath *et al.*, 2001]. We also note that the data points in Figure 3 are subdivided into two subsets referred to as “usual” stations (open symbols) and “unusual” stations (solid symbols); this is discussed in detail below. For each algorithm, the regression lines were fit to all the data. However, if only the data from the usual stations were considered, the algorithm-derived Chl values would show, on average, even higher underestimation at pigment concentrations $>1 \text{ mg m}^{-3}$ than reported above.

[24] Figure 4a compares the OC2 algorithm with our measurements of the chlorophyll concentration, Chl , plotted as a function of the in situ reflectance ratio, $R_{rs}(490)/R_{rs}(555)$. In addition, we show data for the $R_{rs}(442)/R_{rs}(555)$ ratio (Figure 4b). All the surface data collected during the three cruises are shown in this figure. We observe significant scatter of data points about the OC2 curve and systematic overestimation of Chl by OC2 algorithm at low chlorophyll concentrations ($<0.2 \text{ mg m}^{-3}$). Also, the majority of data at intermediate and high pigment concentrations

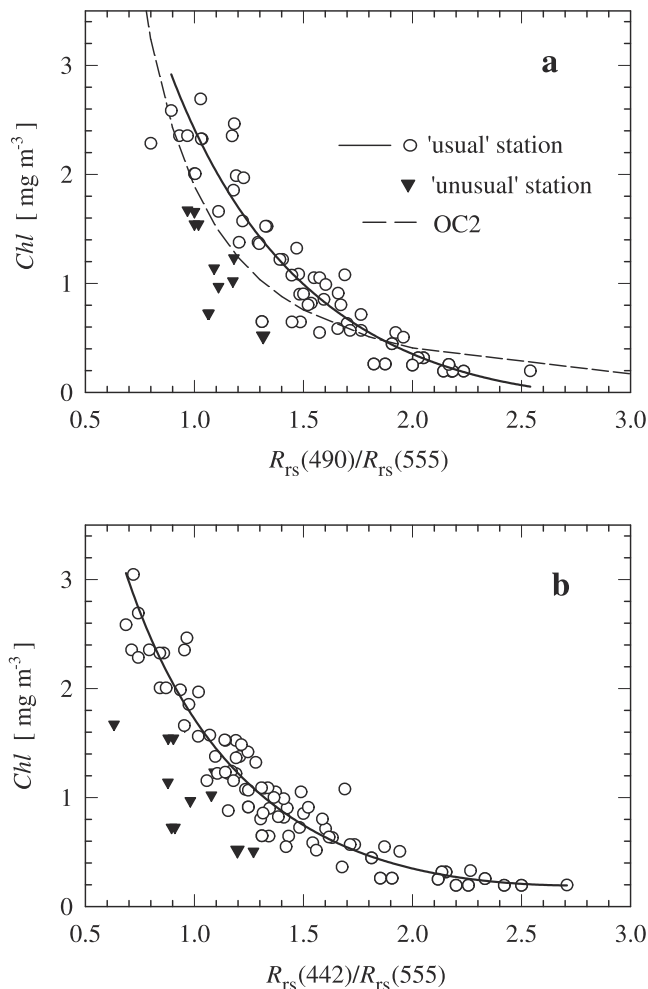


Figure 4. (a) In situ chlorophyll *a* concentration, *Chl*, versus the spectral ratio of remote sensing reflectance, $R_{rs}(490)/R_{rs}(555)$. Solid line is the best fit regression to our data shown as open circles (usual stations). The corresponding equation is $Chl = 2.416 - 9.183 \log_{10}(R_1) + 9.819 \log_{10}^2(R_1)$, where $R_1 = R_{rs}(490)/R_{rs}(555)$, the squared correlation coefficient for log-transformed data, $r^2 = 0.75$, and the number of observations, $n = 54$. Dashed line represents the NASA OC2 (version 4) algorithm [O'Reilly *et al.*, 2000]. Triangles represent data from unusual stations (see text for detailed explanation). (b) Same as Figure 4a but for the reflectance ratio $R_{rs}(442)/R_{rs}(555)$. The best fit equation is $Chl = 1.721 - 6.907 \log_{10}(R_2) + 7.804 \log_{10}^2(R_2)$ where $R_2 = R_{rs}(442)/R_{rs}(555)$, $r^2 = 0.88$ and $n = 79$.

(open circles) show that OC2 tends to underestimate chlorophyll concentration for $Chl > 0.8 \text{ mg m}^{-3}$. The best fit regression lines shown in Figure 4 describe the two-band algorithms that provide the best representation for the majority of data collected in the investigated waters in the summer season (see figure caption for equations). These fits were derived for the data from the usual stations, shown as open circles. The data shown as solid triangles (unusual stations) were excluded from these algorithms (see discussion below). Note that for our data set from the usual stations, the $R_{rs}(442)/R_{rs}(555)$ ratio provides a somewhat better two-band algorithm than the $R_{rs}(490)/R_{rs}(555)$ ratio.

[25] The scatter of data in Figure 4 is seemingly random, but a closer inspection allowed us to identify several data points (triangles) for which the algorithms presented systematically overestimate *Chl*. These data were collected at stations where the measured reflectance spectra had relatively low values of the blue-to-green ratio and a maximum near 510 nm. These data are referred to here as unusual case or unusual stations (we use the term “unusual” because we observed relatively few such reflectance data during the three cruises, but we do not intend to imply that this type of waters is uncommon in the investigated region). In contrast to unusual stations, most of the observed $R_{rs}(\lambda)$ spectra referred to as usual case (open circles in Figure 4) exhibited a maximum at somewhat shorter wavelengths ($\sim 490 \text{ nm}$) and a higher blue-to-green ratio. Figure 5 compares the spectral ratio $R_{rs}(\lambda)/R_{rs}(555)$ for the usual and unusual cases. In each of the two example comparisons, *Chl* is about the same for both the usual and unusual case. This figure clearly shows that two water bodies with the same *Chl* may exhibit significant differences in the spectral shape of R_{rs} . Equation (3) provides a basis for interpreting the observed differences in reflectance. The spectral ratio of absorption coefficient, $a_{w+p}(555)/a_{w+p}(\lambda)$ (for pure water plus particles) shows a difference between the usual and unusual case, which is similar to that of $R_{rs}(\lambda)/R_{rs}(555)$ (Figure 6). The backscattering ratio, $b_b(\lambda)/b_b(555)$, for λ within the blue spectral region, is lower in the unusual case than in the usual case, which suggests that relative contribution to backscattering by water molecules and colloids (relative to larger particles) is smaller in the unusual case than in the usual case. This backscattering behavior reinforces the absorption effect by further reducing the blue-to-green reflectance ratio of the unusual case.

[26] To gain insight into such optical differentiation of waters, we compared the HPLC-derived accessory pigments for the usual and unusual stations occupied on the 1999 cruise. We found that unusual stations showed a relatively high ratio of peridinin to chlorophyll *a*. At these stations the peridinin concentration was 5 to 16% of *Chl*. At usual stations the peridinin concentration was, on average, less than 5% of *Chl*. In addition, in contrast to usual waters, samples of unusual waters showed relatively more 19'-heoxanoyloxyfucoxanthin and less fucoxanthin. The majority of dinoflagellates (Pyrrophyta) contain peridinin as the major carotenoid [Goodwin and Britton, 1988]. In some dinoflagellates, fucoxanthin and/or fucoxanthin derivative such as 19'-heoxanoyloxyfucoxanthin replaces peridinin as the major carotenoid [Jeffrey *et al.*, 1975]. Also, 19'-heoxanoyloxyfucoxanthin is a major or minor pigment in several prymnesiophytes. For example, in the coccolithophorid *Emiliania huxleyi*, fucoxanthin is replaced by 19'-heoxanoyloxyfucoxanthin [Hibberd, 1980]. In addition, the pigment data suggest that diatoms were much more important at the usual stations where we observed significantly higher fucoxanthin/*Chl a* ratio and lower *Chl c3/Chl a* ratio than at the unusual stations (see caption of Figure 5). These differences in pigments are indicative of changes in phytoplankton species composition, which could be responsible, at least partly, for the observed differences in the IOPs and reflectance spectra. It appears that while the usual stations were likely dominated by diatoms, the unusual stations were dominated by dinoflagellates and/or prymnesiophytes.

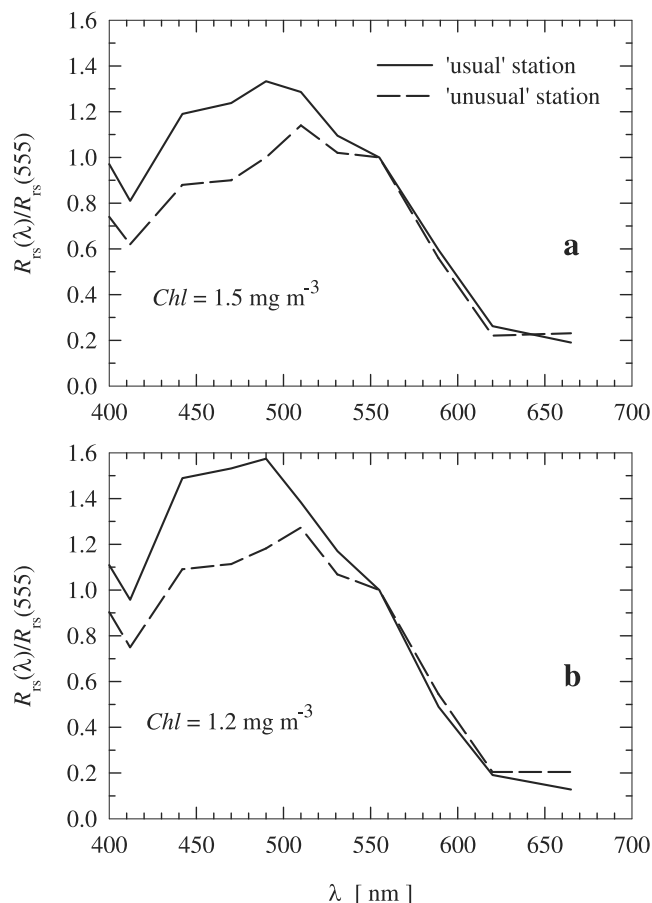


Figure 5. Comparison of the spectral ratio of remote-sensing reflectance, $R_{rs}(\lambda)/R_{rs}(555)$, for the usual (solid line) and unusual (dashed line) case. Two examples are shown from stations occupied on the 1999 cruise. (a) Usual station (70°N , 14°E) and unusual station ($77^{\circ}20.8'$, 8°E). The pigment ratios from the HPLC analysis for the usual and unusual stations, respectively, were $\text{Chl } c_3/\text{Chl } a = 0.056$ and 0.15 , $\text{Fucox}/\text{Chl } a = 0.58$ and 0.29 , $\text{Peridinin}/\text{Chl } a = 0.008$ and 0.16 , $\text{Hexfucox}/\text{Chl } a = 0.13$ and 0.57 . (b) Usual station (70°N , 15°E) and unusual station (78°N , 5°E). The pigment ratios for the usual and unusual stations, respectively, were $\text{Chl } c_3/\text{Chl } a = 0.062$ and 0.17 , $\text{Fucox}/\text{Chl } a = 0.48$ and 0.34 , $\text{Peridinin}/\text{Chl } a = 0.022$ and 0.056 , $\text{Hexfucox}/\text{Chl } a = 0.32$ and 0.51 . In each example comparison, Chl ($\text{Chl } a$) is about the same for the usual and unusual station, as indicated.

Although we have no detailed taxonomic examination to make further analysis, it is interesting to note that data of *Sathyendranath et al.* [2001] suggest similar effects of phytoplankton composition on ocean reflectance in the Labrador Sea.

4.3. Bio-Optical Relationships

4.3.1. Total Absorption Coefficient

[27] The total absorption coefficient, $a(\lambda)$, of surface waters often dominates the variability of the remote sensing reflectance, $R_{rs}(\lambda)$, and the diffuse attenuation coefficient of downwelling irradiance, $K_d(\lambda)$. In our field experiments we did not have a capability to measure $a(\lambda)$ in situ. We derived this coefficient from our in-water measurements of the

backscattering coefficient and reflectance using a model based on numerical simulations of radiative transfer in the ocean surface waters [Stramska et al., 2000]. This model shows that the absorption coefficient in the spectral range 400–490 nm can be estimated from the relationship

$$a(\lambda) = [b_b(\lambda) + 0.0002]/[11.3335 R_{rs}(\lambda)]^{-1}. \quad (8a)$$

A similar relationship was established for the green spectral range (500–560 nm),

$$a(\lambda) = [b_b(\lambda) + 0.0003]/[10.8764 R_{rs}(\lambda)]^{-1}. \quad (8b)$$

We used these relationships to derive $a(\lambda)$ in the spectral range 442–555 nm. The errors in the derived $a(\lambda)$ are usually less than 10% provided that accurate values of b_b and R_{rs} are known [Stramska et al., 2000]. The accuracy of our estimates of $a(\lambda)$ thus depends on errors in the measured values of b_b and R_{rs} . Other possible sources of error include some (albeit small) mismatch in time and location between the b_b and R_{rs} measurements, differences in water volumes sampled by instruments for measuring b_b and R_{rs} , and optical inhomogeneity of the measured water column (as the model was developed for an optically homogeneous ocean).

[28] In order to evaluate the quality of the derived estimates of $a(\lambda)$, we compared these estimates with the measured $K_d(\lambda)$ in the near-surface layer of water column (Figure 7). From radiative transfer simulations the following

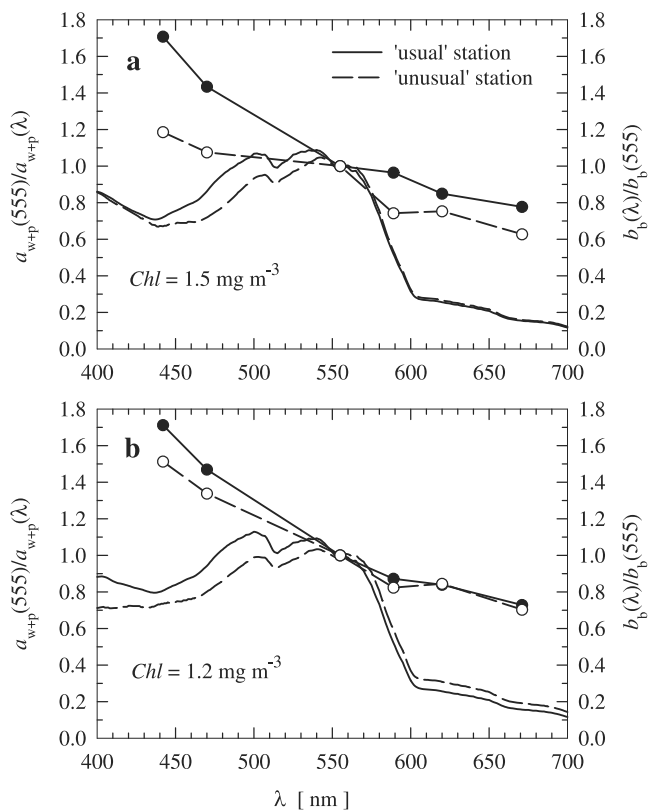


Figure 6. Same as Figure 5, but the comparison is shown for the spectral ratio of absorption by pure seawater plus particles, $a_{w+p}(555)/a_{w+p}(\lambda)$, and the spectral ratio of backscattering coefficient, $b_b(\lambda)/b_b(555)$ (the curves accompanied by data points).

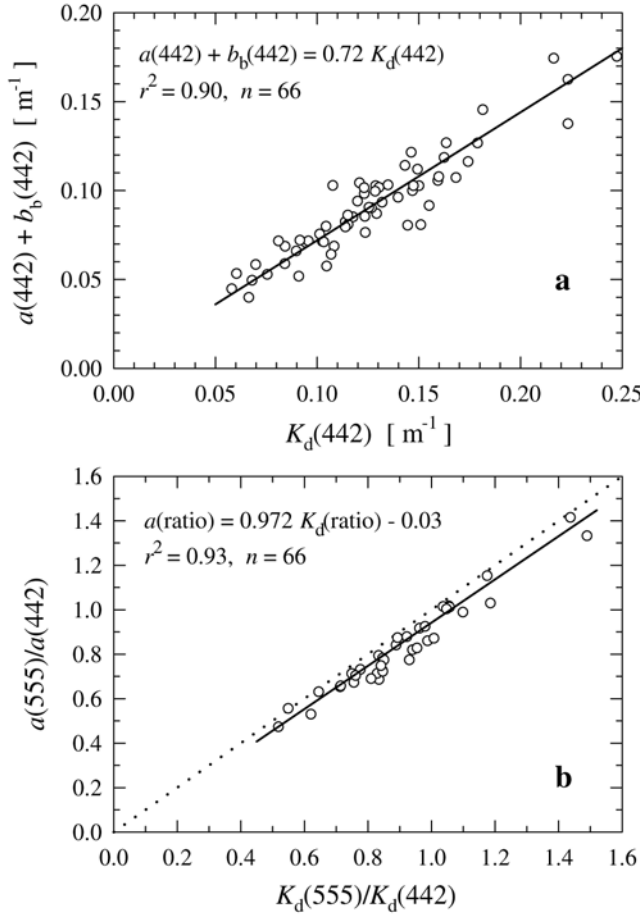


Figure 7. (a) Sum of the total absorption, a , and backscattering, b_b , coefficients versus the diffuse attenuation coefficient of downwelling irradiance, K_d , for light wavelength 442 nm. The absorption coefficient was estimated from the model (see text for details), and b_b and K_d were measured. (b) Absorption ratio, $a(555)/a(442)$, versus the ratio of the diffuse attenuation coefficient, $K_d(555)/K_d(442)$. Solid line is the best linear fit to the data, r^2 is the squared correlation coefficient, and n the number of observations. Dotted line represents $y = x$.

approximate relationship was established by Gordon [1989]:

$$a(\lambda) + b_b(\lambda) = f_1 \mu_d(z = 0^-, \lambda) K_d(\lambda), \quad (9)$$

where $\mu_d(z = 0^-, \lambda)$ is the average cosine for the downwelling light just below the sea surface and f_1 is a factor which accounts for possible changes of μ_d with water depth. It was shown that for the near-surface $K_d(\lambda)$, f_1 is about 1.0395, and for $K_d(\lambda)$ averaged over the entire euphotic zone, f_1 is about 0.93. We estimated that for our data at $\lambda = 442$ nm, the product $f_1 \mu_d(z = 0^-, \lambda)$ is approximately 0.72, which represents a realistic value for our geographic location (Figure 6a). When we plot $a(555)/a(442)$ versus $K_d(555)/K_d(452)$, the data points closely follow the $y = x$ line (Figure 6b), which also suggests that our estimates of $a(\lambda)$ are realistic and subject to only a small error.

[29] In order to illustrate the impact of total absorption on the blue-to-green reflectance ratio used in the chlorophyll algorithm, the $a(555)/a(442)$ and $a(555)/a(490)$ ratios are plotted as a function of Chl in Figure 8. The best fit regression lines show that these ratios decrease substantially with the increase in Chl . The values of the slope parameter of the fitted power function in Figure 8 are significantly smaller than zero, which indicates that the green-to-blue absorption ratio is an important factor driving the decrease of the blue-to-green reflectance ratio with Chl .

4.3.2. Particulate Absorption

[30] Following the approach of Bricaud *et al.* [1998] we approximated the relationship between $a_p(\lambda)$ and Chl by a power function,

$$a_p(\lambda) = A_p(\lambda) Chl^{E_p(\lambda)}, \quad (10)$$

where $A_p(\lambda)$ and $E_p(\lambda)$ were derived by least squares fits on the log-transformed data. The spectral values of these coefficients are plotted in Figure 9, and these results were obtained from data covering the range of Chl from about 0.08 to 5 mg m⁻³.

[31] The variations of $a_p(\lambda)$ as a function of Chl for the three wavelengths (442, 490, and 555 nm) corresponding to the blue/green bands of the SeaWiFS sensor are shown in

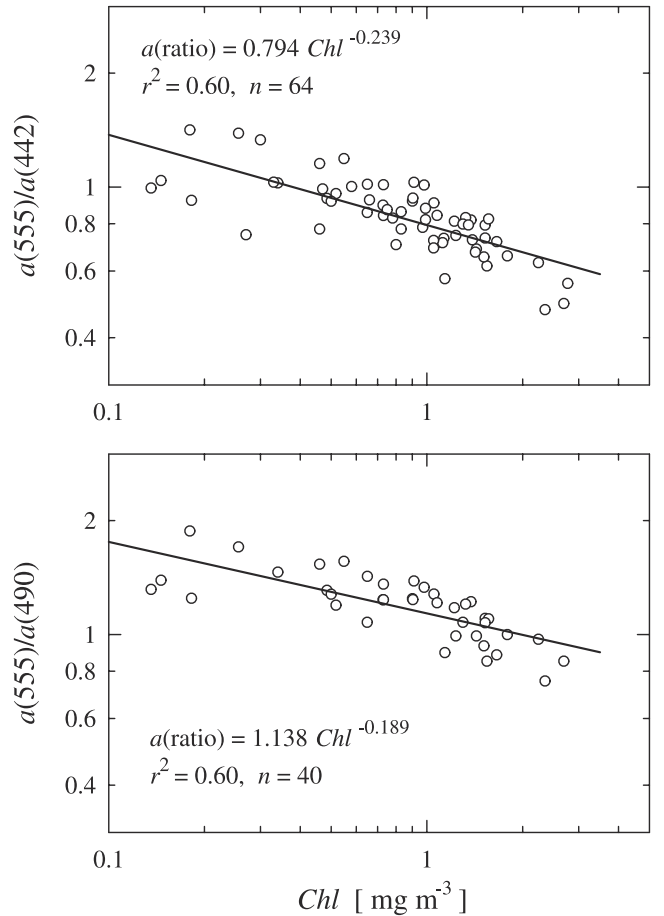


Figure 8. Absorption ratios $a(555)/a(442)$ and $a(555)/a(490)$ as a function of chlorophyll a concentration, Chl . Data (open circles), the least squares fit (solid lines and equations), the r^2 coefficient for log-transformed data, and the number of observations (n) are shown.

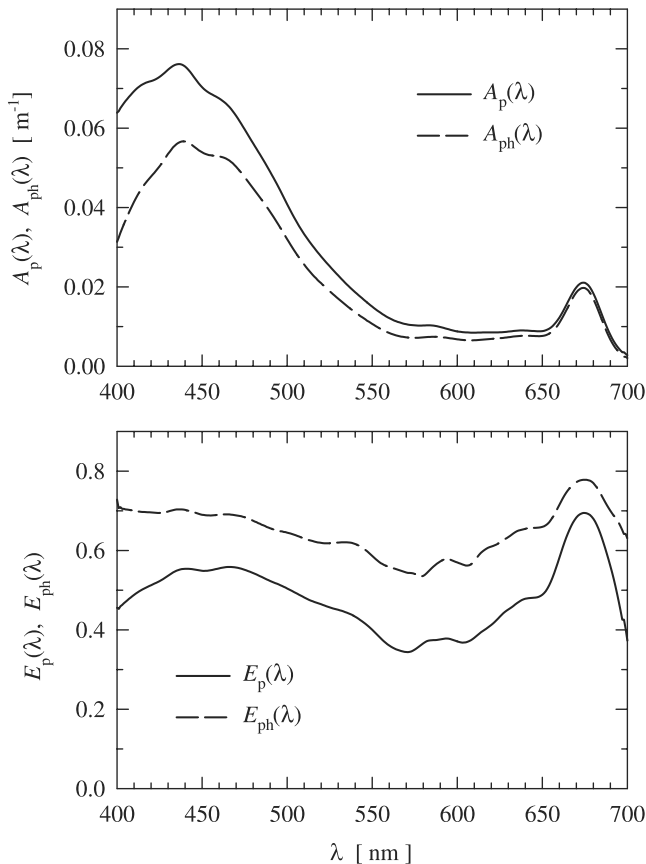


Figure 9. Solid lines show the coefficients, $A_p(\lambda)$ and $E_p(\lambda)$, of power function (equation (10)) describing particulate absorption, $a_p(\lambda)$, as a function of chlorophyll a concentration, Chl . The values of the squared correlation coefficient (not shown) are lowest in the 560–610 nm spectral region (r^2 between 0.35 and 0.4) and highest in the blue and red spectral regions corresponding to chlorophyll a absorption bands (r^2 in the range 0.6–0.75). Dashed lines show the coefficients, $A_{ph}(\lambda)$ and $E_{ph}(\lambda)$, of power function (equation (11)) describing phytoplankton absorption, $a_{ph}(\lambda)$, as a function of chlorophyll a concentration, Chl . The r^2 values are fairly uniform (0.6–0.8) throughout the visible spectrum. All coefficients were obtained by linear regression on log-transformed data.

Figure 10. For the examined range of Chl , a_p at these wavelengths varied by about 1 order of magnitude. Nearly all our data points in the blue spectral region are above the regression lines of *Bricaud et al.* [1998], which are based on a large data set from mid and low latitudes. This indicates that the chlorophyll-specific particulate absorption, $a_p^*(\lambda)$, in the blue is, on average, higher in the investigated polar waters compared to the *Bricaud et al.* data from lower latitudes. The result is somewhat different at 555 nm, where many of our data points for $Chl > 0.5 \text{ mg m}^{-3}$ are located around the *Bricaud et al.* line. Our estimates of $a_p^*(\lambda)$ in the blue are also higher than those obtained by *Mitchell* [1992] in the north polar waters of the Barents Sea and Fram Strait.

[32] While our absorption coefficients were normalized to chlorophyll a from spectrophotometric measurement which was very similar to the HPLC-derived chlorophyll a (phaeopigments are excluded from our normalization),

the *Mitchell* data were normalized by chlorophyll a plus phaeopigments measured by fluorometry, and the *Bricaud et al.* data were normalized by chlorophyll a plus divinyl chlorophyll a and phaeophytin a obtained by various methods. The higher values of $a_p^*(\lambda)$ observed in our data set could be partly attributed to these methodological differences. For example, fluorometric determinations often yield higher values of chlorophyll a (lower estimates of chlorophyll-specific absorption) compared to HPLC determinations, which was also observed on our 1999 cruise. Regardless of these methodological issues, we note that the increase in the particulate absorption per unit of chlorophyll a , especially in the blue spectral region, may be caused by such factors as an increase in the contribution of accessory pigments, decrease in the pigment package effect, and/or increase in the contribution of detrital absorption.

[33] Figure 11 shows the green-to-blue ratio for the absorption by pure seawater and particles (a_{w+p}) as a function of Chl . For both pairs of wavelengths, 555/442 nm and 555/490 nm, there is a good correlation between the a_{w+p} ratios and Chl . These relationships are steeper than those for total absorption shown in Figure 8. This indicates that the chlorophyll algorithm based on the decrease of the blue-to-green reflectance ratio with Chl is driven largely by a decrease in the green-to-blue ratio of absorption by pure water and particles.

4.3.3. Absorption by Phytoplankton

[34] Phytoplankton were the dominant component of particulate absorption in the waters investigated. On average, phytoplankton contributed 74, 77, and 70% to a_p at 442, 490, and 555 nm, respectively. The total particulate and phytoplankton absorption were highly correlated in the blue ($r^2 = 0.92$ and 0.91 at 442 and 490 nm, respectively). In the green, the correlation was not as high but still significant ($r^2 = 0.73$ at 555 nm). Similarly to $a_p(\lambda)$, we fitted the data of phytoplankton absorption $a_{ph}(\lambda)$ versus Chl to the power function

$$a_{ph}(\lambda) = A_{ph}(\lambda)Chl^{E_{ph}(\lambda)}. \quad (11)$$

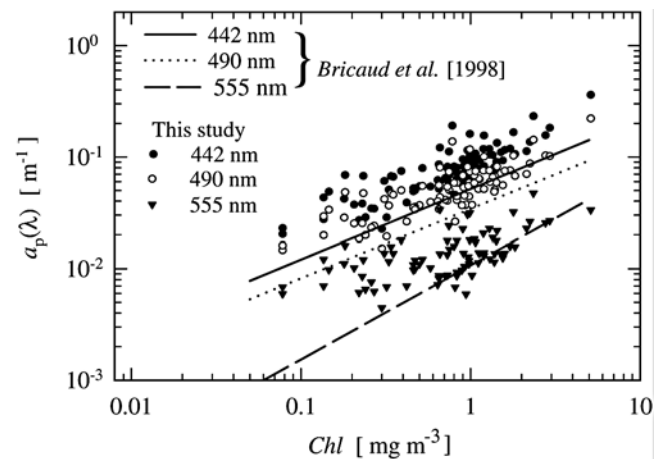


Figure 10. Coefficient of particulate absorption, $a_p(\lambda)$, as a function of chlorophyll a concentration, Chl , for the three wavelengths, 442, 490, and 555 nm. Our data (solid circles, open circles, and triangles) are compared with regression lines from *Bricaud et al.* [1998].

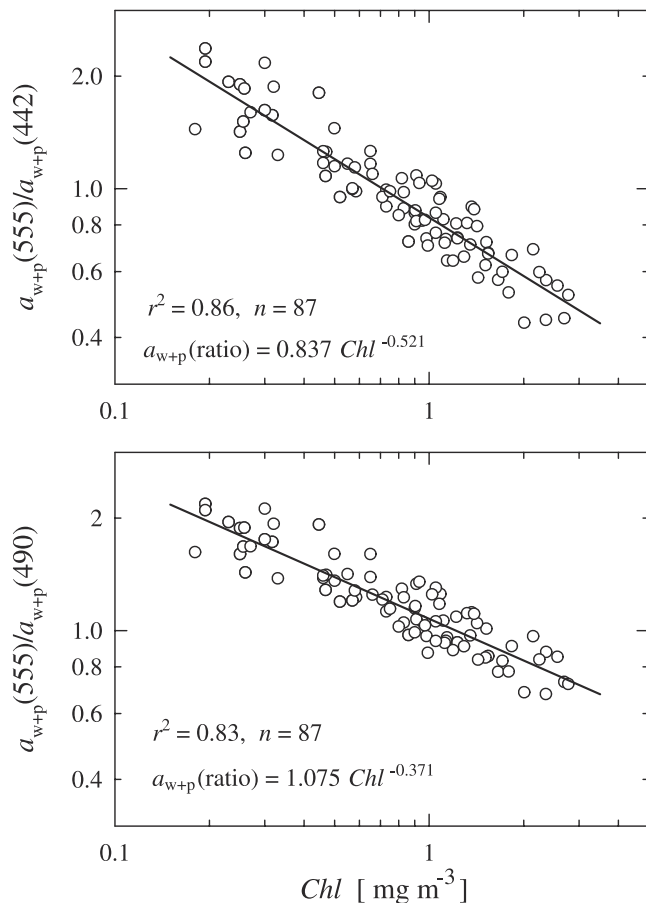


Figure 11. Absorption ratios $a_{w+p}(555/442)$ and $a_{w+p}(555/490)$ as a function of chlorophyll a concentration, Chl . Data (open circles), the least squares fit (solid lines and equations), the r^2 coefficient for log-transformed data, and the number of observations (n) are shown.

The coefficients $A_{ph}(\lambda)$ and $E_{ph}(\lambda)$ are shown in Figure 9. The chlorophyll-specific absorption coefficients of phytoplankton, $a_{ph}^*(\lambda)$, are generally within a range of values reported by *Bricaud et al.* [1995] for their large data set from lower latitudes (not shown here). With increasing Chl , however, our estimates of $a_{ph}^*(\lambda)$ in the blue spectral region tend to be higher than the average values of *Bricaud et al.*

[35] The green-to-blue ratios (555/442 nm and 555/490 nm) of absorption by pure seawater plus phytoplankton (a_{w+ph}) as a function of Chl (not shown here) exhibit a similar pattern to that for pure water and particles illustrated in Figure 11. The differences are that the values of the a_{w+ph} ratios are generally somewhat higher than the values of the a_{w+p} ratios, and the relationships for the a_{w+ph} ratios versus Chl have slightly steeper slopes and higher values of the squared correlation coefficient than the relationships for the a_{w+p} ratios. This indicates that a decrease in the green-to-blue ratio of absorption by pure water and phytoplankton with Chl was a major factor controlling the decrease of the blue-to-green reflectance ratio with Chl in the investigated waters.

4.3.4. CDOM Absorption

[36] We did not measure absorption by colored dissolved organic matter (CDOM) on our cruises. However, the

contribution of CDOM can be assessed from a comparison of the estimates of the total absorption coefficient, a , and the sum of water and particulate absorption, a_{w+p} , at 442 nm (Figure 12). The data points scatter around the $y = x$ line without a systematic departure from this line. At most stations $a(442)$ and $a_{w+p}(442)$ are similar, which suggests a small (<10%) contribution of CDOM to $a(442)$. At few stations $a(442)$ is considerably higher than $a_{w+p}(442)$, which implies a significant contribution of CDOM absorption. The data points above the $y = x$ line indicate either the overestimation of the measured $a_p(442)$ or the underestimation of the model-derived $a(442)$. In spite of unavoidable uncertainties in the estimates of $a(442)$ and $a_{w+p}(442)$, it appears that the contribution of a_{CDOM} to the total absorption at 442 nm and longer wavelengths was generally small.

4.3.5. Backscattering Versus Chlorophyll and Reflectance

[37] Equation (2) shows that the total backscattering coefficient, $b_b(\lambda)$, can be expressed as a sum of contributions by pure seawater, $b_{bw}(\lambda)$, and particles, $b_{bp}(\lambda)$. The $b_{bw}(\lambda)$ coefficient is assumed to be known and constant at any given λ . The particulate backscattering $b_{bp}(\lambda)$ is variable and needs to be examined. In the investigated surface waters the contribution of particles to b_b at 555 nm varied between 40 and 80%. The coefficient $b_{bp}(555)$ covaried with Chl (Figure 13a) and the least squares fit provided the following relationship:

$$b_{bp}(555) = 0.0019 Chl^{0.5}. \quad (12)$$

Figure 13a shows that our $b_{bp}(555)$ values for any given Chl are between the regression lines for the Ross Sea and the Antarctic Polar Front Zone APFZ [*Reynolds et al.*, 2001] but are consistently lower than those predicted by the *Morel* [1988] model. Without detailed data describing particle size distribution and types of particles suspended in seawater, interpretation of the regional differences shown in Figure 13a would be speculative. We only mention it because small particles (mainly $<1 \mu\text{m}$ in size) may often dominate backscattering [*Morel and Ahn*, 1991; *Stramski and Kiefer*, 1991], so Figure 13a suggests that the population of

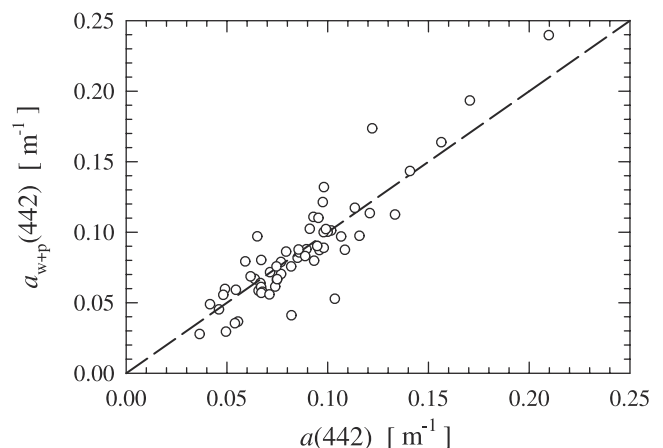


Figure 12. Absorption coefficient by pure seawater plus particles, $a_{w+p}(442)$, obtained from measurements of $a_p(442)$ versus the total absorption coefficient, $a(442)$, estimated from a model (see text for details). Dashed line represents $y = x$.

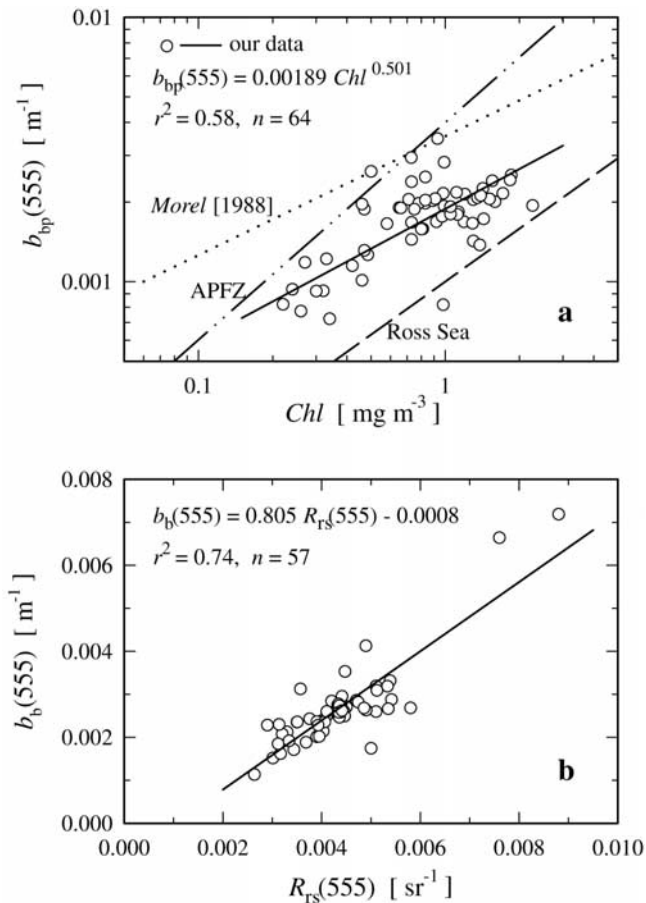


Figure 13. (a) Backscattering coefficient of particles $b_{bp}(555)$ versus chlorophyll a concentration, Chl . For comparison, similar relationships obtained from measurements in the Ross Sea and the Antarctic Polar Front Zone APFZ [Reynolds et al., 2001] and from a bio-optical model [Morel, 1988] are shown. The measurements of Reynolds et al. were processed with an earlier version of Hydrosort software than the version 2.06 used in this study. (b) Total backscattering coefficient $b_b(555)$ versus remote-sensing reflectance, $R_{rs}(555)$. Our data (open circles), the corresponding least squares fit (solid lines and equations), the r^2 coefficient, and the number of observations (n) are shown. r^2 in Figure 13a is for log-transformed data.

particles in the investigated north polar waters could have included relatively more small particles than the Ross Sea and less small particles compared to APFZ.

[38] According to equation (1), the variation in $b_b(\lambda)$ induces a proportional change in R_{rs} . In our data set the correlation between $b_b(\lambda)$ and $R_{rs}(\lambda)$ was greatest in the green spectral region, where the effect of $a(\lambda)$ on $R_{rs}(\lambda)$ is relatively small. The best fit relationship between b_b and R_{rs} at 555 nm is (Figure 13b)

$$b_b(555) = 0.805 R_{rs}(555) - 0.0008. \quad (13)$$

4.3.6. Spectral Dependence of Backscattering

[39] In general the wavelength dependence of backscattering $b_b(\lambda)$ in the ocean reflects relative contributions by water molecules and particles [Morel, 1973; Morel and Gentili,

1991]. Pure water backscattering is characterized by a strong wavelength dependency, $b_{bw}(\lambda) \sim \lambda^{-4.32}$. The spectral dependency for particles is variable and depends on the size distribution and composition of particle population. Models of backscattering usually assume a smooth wavelength dependency for $b_{bp}(\lambda)$, either with a constant slope ($\sim \lambda^{-1}$) or a slope that varies as a function of the parameters characterizing phytoplankton concentration [Carder et al., 1999].

[40] Because our interest is here focused on ocean color algorithms in which reflectance depends on the total backscattering coefficient, we will discuss the spectral shape of $b_b(\lambda)$. Our measurements indicate that the spectral dependency of $b_b(\lambda)$ changed in a systematic way. The steepest slope of the $b_b(\lambda)$ spectrum was observed in waters with low Chl , where low $b_b(\lambda)$ values were observed. Assuming that $b_b(\lambda)$ has the wavelength dependence defined by

$$b_b(\lambda) = [b_{bw}(555) + b_{bp}(555)](\lambda/555)^{-\gamma}, \quad (14)$$

our data indicate that the slope γ is strongly correlated with the magnitude of backscattering at 555 nm (Figure 14). This relationship is best described by the following equation:

$$\gamma = 0.061 b_b(555)^{-0.58}. \quad (15)$$

Our calculations also indicate that if $b_b(555)$ is known from measurements, the backscattering coefficient at other wavelengths in the investigated waters can be estimated with an error of less than 10% from equations (14) and (15).

[41] To provide further insight into the interpretation of the two-band chlorophyll algorithms, we plotted the blue-to-green backscattering ratios, $b_b(442)/b_b(555)$ and $b_b(490)/b_b(555)$, as a function of Chl (Figure 15). In this data set, Chl changes nearly 30-fold, but the overall variations of the values of backscattering ratio are relatively small, that is, a factor of 1.6 and 1.3 for $b_b(442)/b_b(555)$ and $b_b(490)/b_b(555)$, respectively. This result indicates that the backscattering ratio was less important than the absorption ratio in driving the decrease of the blue-to-green reflectance ratio with Chl . Note also that our backscattering ratios are higher than those predicted from the model of Carder et al. [1999].

4.4. Absorption Algorithm

[42] Although in-water ocean color algorithms are mostly focused on the retrieval of chlorophyll a , it has been shown that the ocean optical properties can also be derived from water-leaving radiance or remote-sensing reflectance [e.g., Austin and Petzold, 1981; Lee et al., 1998; Carder et al., 1999; Barnard et al., 1999; Loisel et al., 2001]. We will now examine relationships between the band ratios of R_{rs} and the total absorption and phytoplankton absorption coefficients at 442 nm. Our data show that the absorption coefficients at 442 nm and other wavelengths are more or less correlated. For example, we obtained the following relationships:

$$a(490) = 0.5914 a(442) + 0.0102 \quad (r^2 = 0.96, n = 41) \quad (16a)$$

$$a(555) = 0.2702 a(442) + 0.0464 \quad (r^2 = 0.7, n = 66). \quad (16b)$$

Similar relationships were observed in data sets collected in oceanic waters at lower latitudes [Barnard et al., 1998, 1999].

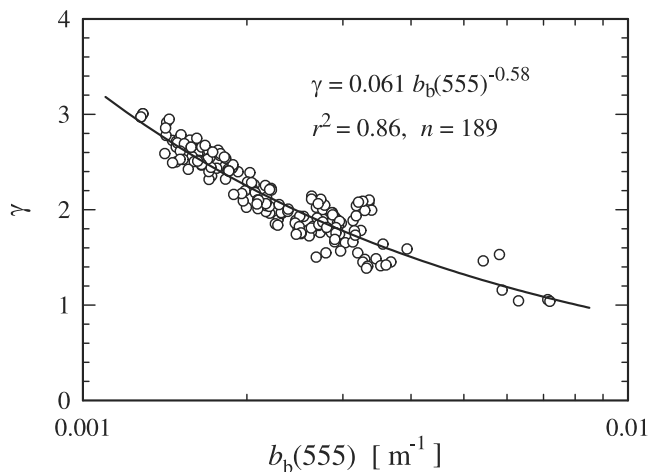


Figure 14. Slope parameter γ from equation (14) versus the total backscattering coefficient b_b at 555 nm. Data (open circles), the least squares fit (solid line and equation), the r^2 coefficient for log-transformed data, and the number of observations (n) are shown.

[43] Our data for $a(442)$ show a good correlation with the $R_{rs}(442)/R_{rs}(555)$ and $R_{rs}(490)/R_{rs}(555)$ ratios (Figure 16). This suggests that $a(442)$ can be estimated from remote sensing with a good accuracy using a simple two-band algorithm. For this purpose, the $R_{rs}(442)/R_{rs}(555)$ ratio is better than $R_{rs}(490)/R_{rs}(555)$, which is similar to what we found in the case of chlorophyll algorithm. The spread of data in the relationship between the phytoplankton absorption $a_{ph}(442)$ and reflectance ratios is larger than that for total absorption, although the correlation is still good (Figure 17). The reduced correlation for phytoplankton absorption is understandable because R_{rs} is a stronger function of the total absorption than absorption by any individual component and water bodies with the same a can have different contributions of the a_{ph} , a_d , and a_{CDOM} components.

[44] For comparison, Figures 16a and 17a include other empirical algorithms based on the $R_{rs}(490)/R_{rs}(555)$ ratio, which were developed by Lee *et al.* [1998] using data from lower latitudes. For the same $R_{rs}(490)/R_{rs}(555)$, our relationships lead to lower values of $a(442)$ and higher values of $a_{ph}(442)$ than those predicted from the Lee *et al.* algorithms. The total absorption given by Lee *et al.* [1998] was estimated from a method that differs from our approach in this study. The phytoplankton absorption was, however, determined from the same filter-pad technique, although the β correction of Lee *et al.* [1998] differs from our correction. These methodological differences could be, to some extent, responsible for the observed differences between our data and the Lee *et al.* algorithms, but the real differences in the absorption properties of water bodies studied in this work and in the work of Lee *et al.* [1998] are probably important to this comparison as well.

5. Conclusions

[45] The best two-band algorithm for chlorophyll a based on our data from the north polar region of Atlantic involves the reflectance ratio $R_{rs}(442)/R_{rs}(555)$ (Figure 4b). This

algorithm yields chlorophyll concentrations that can differ significantly from those obtained from the standard empirical NASA algorithms (OC2, OC4, and chlor-MODIS) developed from a large database dominated by measurements from lower latitudes. Our measurements indicate that the NASA algorithms would overpredict Chl at low pigment concentrations (a factor of 2 for $Chl < 0.2 \text{ mg m}^{-3}$) and underpredict Chl at higher concentrations (by 20% or more at 3 mg m^{-3}) in the investigated waters hypothesized to be dominated by diatoms. In these waters, we observed a relatively high green-to-blue absorption ratio and a relatively high blue-to-green backscattering ratio, which both contributed to a relatively high blue-to-green reflectance ratio (compared to data from lower latitudes) at intermediate and high chlorophyll concentrations. This feature of reflectance has been previously observed in the north polar waters and was attributed primarily to low values of chlorophyll-specific absorption of phytoplankton in the blue spectral region [Mitchell, 1992; Sathyendranath *et al.*, 2001]. It was suggested that these low values are caused by a strong package effect in large phytoplankton (mainly diatom) cells

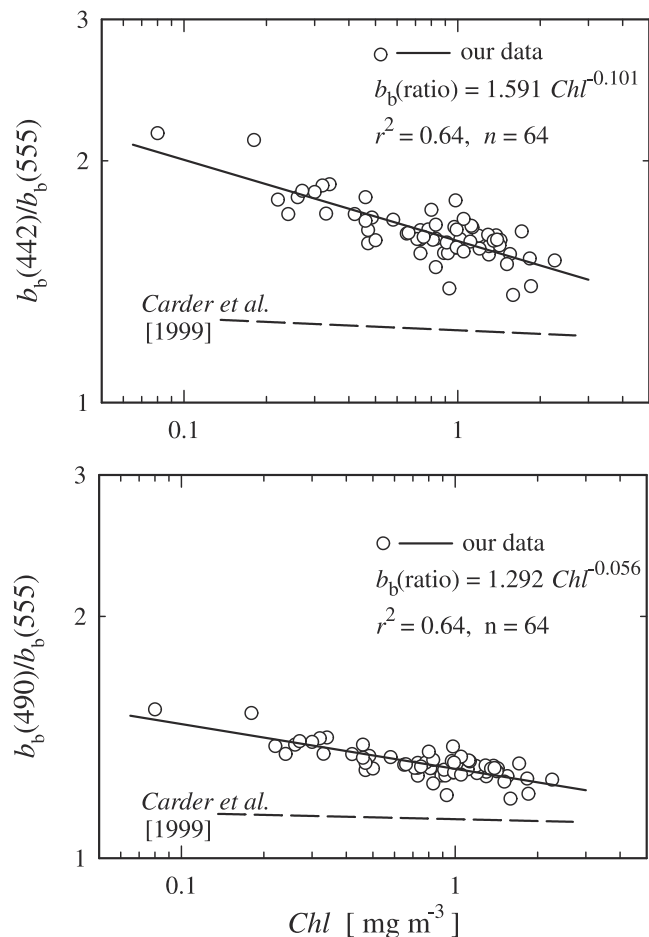


Figure 15. Backscattering ratios $b_b(442/555)$ and $b_b(490/555)$ as a function of chlorophyll a concentration, Chl (open circles). For comparison, the backscattering ratios estimated from a semianalytic model of Carder *et al.* [1999] are also shown (dashed lines). If applied to our study region, this model would underestimate $b_b(442)/b_b(555)$ by over 30% and $b_b(490)/b_b(555)$ by 20% for $Chl < 0.2 \text{ mg m}^{-3}$.

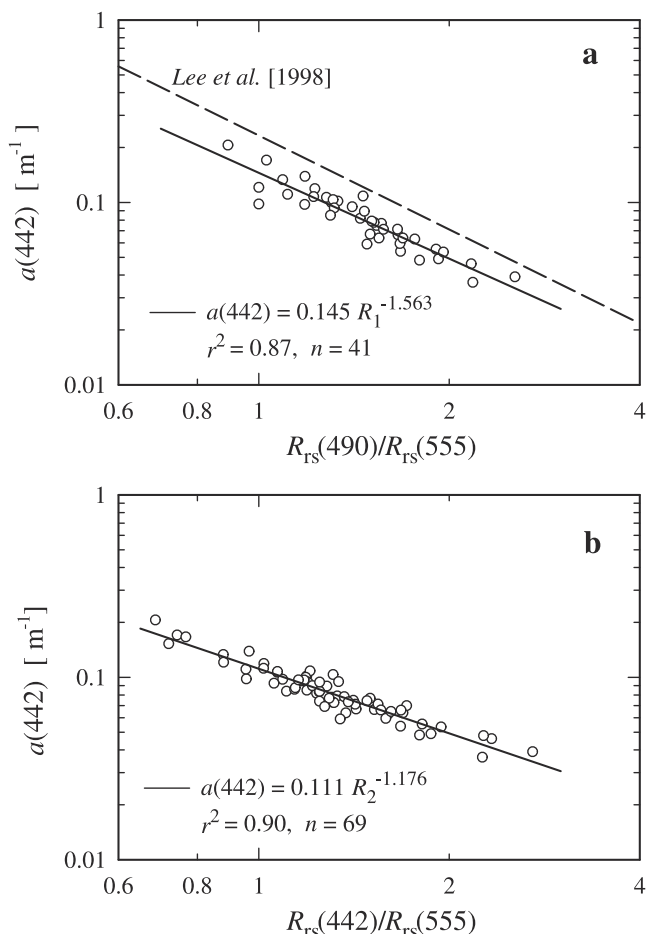


Figure 16. Relationships between the total absorption coefficient at 442 nm and the blue-to-green ratio of remote-sensing reflectance. (a) $a(442)$ versus $R_{rs}(490)/R_{rs}(555)$. (b) $a(442)$ versus $R_{rs}(442)/R_{rs}(555)$. Data (open circles), the least squares fit (solid lines and equations), the r^2 coefficient for log-transformed data, and the number of observations (n) are shown. For comparison, the empirical algorithm derived by Lee *et al.* [1998] is shown (dashed line). This algorithm was actually derived for $a(440)$ rather than $a(442)$ but this difference is insignificant.

whose intracellular pigment concentrations are high due to acclimation to relatively low irradiances at high latitudes. In addition, under low light the cells contain smaller amounts of photoprotective accessory pigments, which further reduces the chlorophyll-specific absorption in the blue.

[46] Interestingly, our measurements do not reveal any systematic reduction in the chlorophyll-specific absorption of particles and phytoplankton compared to low- and mid-latitude data. Our data show that the relatively high blue-to-green reflectance ratio in waters hypothetically dominated by diatoms is associated with both absorption and backscattering properties of the water. In such waters, we observed an enhanced green-to-blue absorption that may be related to relatively small contribution of CDOM absorption (and possibly detritus) and an enhanced blue-to-green backscattering ratio that may be related to relatively large contribution of water molecules (and possibly colloidal particles) to backscattering. The distinct differentiation of our optical data between water types referred to as “usual”

(hypothetically dominated by diatoms) and “unusual” (hypothetically dominated by dinoflagellates and/or prymnesiophytes) (see Figures 5 and 6) provide an example of significance of variations in phytoplankton species composition for remote sensing of chlorophyll a . This underscores a need for a regional/seasonal approach to ocean color algorithm development and applications.

[47] The measurements of the absorption and backscattering coefficients allowed us to develop an understanding of the patterns in our data that describe the two-band algorithms for chlorophyll a . In this regard, we can draw two major conclusions. First, the general trend of the decrease in the blue-to-green reflectance ratio with Chl (i.e., the two-band algorithm for chlorophyll a) was driven primarily by the variation in the green-to-blue absorption ratio as a function of Chl (Figures 8 and 11). The changes of the blue-to-green backscattering ratio with Chl were also significant but relatively smaller than those of the absorption ratio (Figure 15). In the absorption variability, particles, especially phytoplankton, were of major importance and CDOM was of minor importance. Second, the seemingly random scatter of data points about the general trend line of the chlorophyll two-band algorithm is caused by variations in absorption and backscattering at any given Chl (Figures 8, 11, and 15). In our data set, these seemingly random variations in absorption appear to have a greater impact than

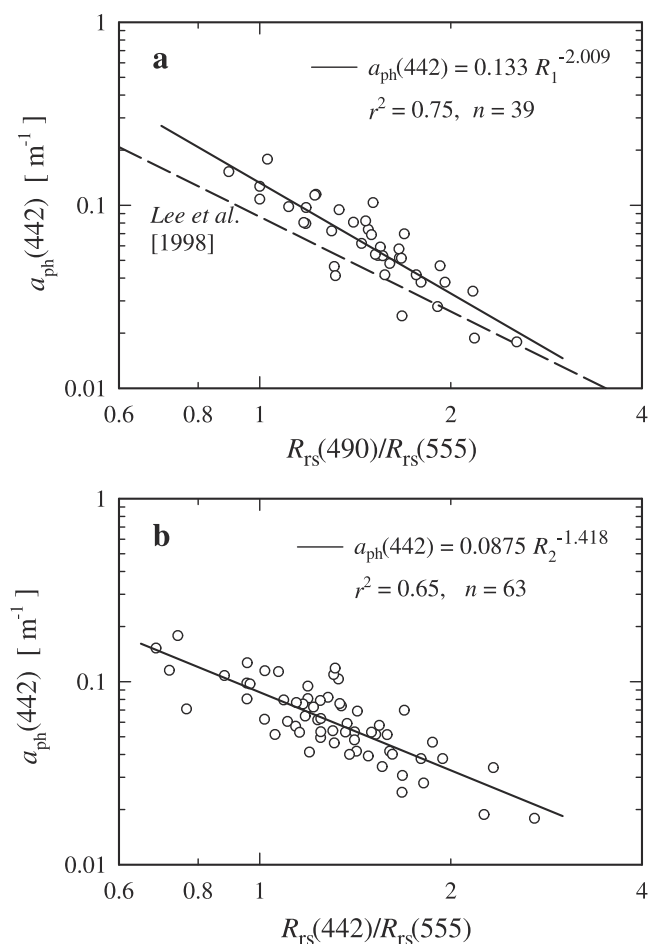


Figure 17. Same as Figure 16 but for phytoplankton absorption coefficient.

variations in backscattering. Clearly, there is a need for a better understanding of the substantial variability in the absorption and backscattering per unit of chlorophyll *a* concentration in ocean waters.

[48] **Acknowledgments.** Financial support for this research was provided by NASA Grants NAG5-6512 and NAG5-6466 (awarded to M.S. and D.S.) of the EOS Validation Program, and by Polish Academy of Sciences (R.H., S.K., and J.S.). Partial support was also provided by NATO Collaborative Linkage Grant (EST.CLG.975231). The oceanographic cruises were supported by Institute of Oceanology, Polish Academy of Sciences. We thank Polish colleagues participating in the cruises as well as the officers and crews of the R/V *Oceania* for assistance in the collection of field data and logistical support. We also thank J. Wieland for making the HPLC analysis and A. Dickson for comments on the manuscript.

References

- Austin, R. W., and T. J. Petzold, The determination of the diffuse attenuation coefficient of sea water using Coastal Zone Colour Scanner, in *Oceanography from Space*, edited by J. F. R. Grower, pp. 239–256, Plenum, New York, 1981.
- Babin, M., and D. Stramski, Light absorption by aquatic particles in the near-infrared spectral region, *Limnol. Oceanogr.*, *47*, 911–915, 2002.
- Barnard, A. H., W. S. Pegau, and J. R. V. Zaneveld, Global relationships of the inherent optical properties of the oceans, *J. Geophys. Res.*, *103*, 24,955–24,968, 1998.
- Barnard, A. H., J. R. V. Zaneveld, and W. S. Pegau, In situ determination of the remotely sensed reflectance and the absorption coefficient: closure and inversion, *Appl. Opt.*, *38*, 5108–5117, 1999.
- Bricaud, A., and D. Stramski, Spectral absorption coefficients of living phytoplankton and non-algal biogenous matter: A comparison between the Peru upwelling area and Sargasso Sea, *Limnol. Oceanogr.*, *35*, 562–582, 1990.
- Bricaud, A., M. Babin, A. Morel, and H. Claustre, Variability in the chlorophyll-specific absorption coefficients of natural phytoplankton: Analysis and parameterization, *J. Geophys. Res.*, *100*, 13,321–13,332, 1995.
- Bricaud, A., A. Morel, M. Babin, K. Allali, and H. Claustre, Variations of light absorption by suspended particles with chlorophyll *a* concentration in oceanic (case 1) waters: Analysis and implications for bio-optical models, *J. Geophys. Res.*, *103*, 31,033–31,044, 1998.
- Carder, K. L., S. K. Hawes, K. A. Baker, R. C. Smith, R. G. Steward, and B. G. Mitchell, Reflectance model for quantifying chlorophyll *a* in the presence of productivity degradation products, *J. Geophys. Res.*, *96*, 20,599–20,611, 1991.
- Carder, K. L., F. R. Chen, Z. P. Lee, and S. K. Hawes, Semianalytic Moderate-Resolution Imaging Spectrometer algorithms for chlorophyll *a* and absorption with bio-optical domains based on nitrate-depletion temperatures, *J. Geophys. Res.*, *104*, 5403–5421, 1999.
- Cleveland, J. S., and A. D. Weidemann, Quantifying absorption by aquatic particles: A multiple scattering correction for glass-fiber filters, *Limnol. Oceanogr.*, *38*, 1321–1327, 1993.
- Cota, G. F., Remote sensing of ocean color in the Arctic: Algorithm development and comparative validation, *NASA Tech. Memo. 2001-209976*, 65–70, 2001.
- Dierssen, H. M., and R. C. Smith, Bio-optical properties and remote sensing ocean color algorithms for Antarctic Peninsula waters, *J. Geophys. Res.*, *105*, 26,301–26,312, 2000.
- Esaias, W. E., et al., An overview of MODIS capabilities for ocean science observations, *IEEE Trans. Geosci. Remote Sens.*, *36*, 1250–1265, 1998.
- Esaias, W. E., R. L. Iverson, and K. Turpie, Ocean province classification using ocean colour data: Observing biological signatures of variations in physical dynamics, *Global Change Biol.*, *6*, 39–55, 2000.
- Fenton, N., J. Priddle, and P. Tett, Regional variations in biooptical properties of surface waters in the Southern Ocean, *Antarct. Sci.*, *6*, 443–448, 1994.
- Goericke, R., and D. J. Repeta, Chlorophyll-*a* and chlorophyll-*b* and divinyl chlorophyll-*a* and chlorophyll-*b* in the open subtropical North-Atlantic Ocean, *Mar. Ecol. Prog. Ser.*, *101*, 307–313, 1993.
- Goodwin, T. W., and G. Britton, Distribution and analysis of carotenoids, in *Plant Pigments*, edited by T. W. Goodwin, pp. 61–132, Academic, San Diego, Calif., 1988.
- Gordon, H. R., Can the Lambert law be applied to the diffuse attenuation coefficient of ocean water?, *Limnol. Oceanogr.*, *34*, 1389–1409, 1989.
- Gordon, H. R., Atmospheric correction of ocean color imagery in the Earth Observing System era, *J. Geophys. Res.*, *102*, 17,081–17,106, 1997.
- Gordon, H. R., and A. Morel, *Remote Assessment of Ocean Color for Interpretation of Satellite Visible Imagery-A Review*, 114 pp., Springer-Verlag, New York, 1983.
- Gordon, H. R., and M. Wang, Retrieval of water-leaving radiance and aerosol optical thickness over the oceans with SeaWiFS: A preliminary algorithm, *Appl. Opt.*, *33*, 443–452, 1994.
- Gordon, H. R., O. B. Brown, R. H. Evans, J. W. Brown, R. C. Smith, K. S. Baker, and D. K. Clark, A semianalytical radiance model of ocean color, *J. Geophys. Res.*, *93*, 10,909–10,924, 1988.
- Hibberd, D. J., Prymnesiophytes (=Haptophytes), in *Phytoflagellates*, *Dev. Mar. Biol.*, vol. 2, edited by E. R. Cox, pp. 273–317, Elsevier, New York, 1980.
- Hooker, S. B., and C. R. McClain, The calibration and validation of SeaWiFS data, *Prog. Oceanogr.*, *45*, 427–465, 2000.
- Hooker, S. B., N. W. Rees, and J. Aiken, An objective methodology for identifying oceanic provinces, *Prog. Oceanogr.*, *45*, 313–338, 2000.
- Jeffrey, S. W., M. Sielicki, and F. T. Haxo, Chloroplast pigment patterns in dinoflagellates, *J. Phycol.*, *11*, 374–384, 1975.
- Lee, Z., K. L. Carder, S. K. Hawes, R. G. Steward, T. G. Peacock, and C. O. Davis, A model for interpretation of hyperspectral remote-sensing reflectance, *Appl. Opt.*, *33*, 5721–5732, 1994.
- Lee, Z. P., K. L. Carder, R. G. Steward, T. G. Peacock, C. O. Davis, and J. S. Patch, An empirical algorithm for light absorption by ocean water based on color, *J. Geophys. Res.*, *103*, 27,967–27,978, 1998.
- Loisel, H., D. Stramski, B. G. Mitchell, F. Fell, V. Fournier-Sicre, B. Lemasle, and M. Babin, Comparison of the ocean inherent optical properties obtained from measurements and inverse modeling, *Appl. Opt.*, *40*, 2384–2397, 2001.
- Longhurst, A., S. Sathyendranath, T. Platt, and C. Caverhill, An estimate of global primary production in the ocean from satellite radiometer data, *J. Plankton Res.*, *17*, 1245–1271, 1995.
- Maffione, R. A., and D. R. Dana, Instruments and methods for measuring the backward-scattering coefficient of ocean waters, *Appl. Opt.*, *36*, 6057–6067, 1997.
- Marker, A. F. H., E. A. Nusch, H. Rai, and B. Riemann, The measurement of photosynthetic pigments in freshwaters and standardisation of methods: Conclusions and recommendations, *Arch. Hydrobiol. Beih. Ergebn. Limnol.*, *14*, 91–106, 1980.
- McClain, C. R., M. L. Cleave, G. C. Feldman, W. W. Gregg, and S. B. Hooker, Science quality SeaWiFS data for global biosphere research, *Sea Technol.*, *39*, 10–16, 1998.
- Mitchell, B. G., Algorithm for determining the absorption coefficient of aquatic particulates using the quantitative filter technique (QFT), in *Ocean Optics X*, edited by R. W. Spinrad, *Proc. SPIE Int. Soc. Opt. Eng.*, *1302*, 137–148, 1990.
- Mitchell, B. G., Predictive bio-optical relationships for polar oceans and marginal ice zones, *J. Mar. Syst.*, *3*, 91–105, 1992.
- Mitchell, B. G., and O. Holm-Hansen, Bio-optical properties of Antarctic Peninsula waters: Differentiation from temperate ocean models, *Deep Sea Res.*, *38*, 1009–1028, 1991.
- Mitchell, B. G., et al., Determination of spectral absorption coefficients of particles, dissolved material and phytoplankton for discrete water samples, *NASA Tech. Memo. 2000-209966*, 125–153, 2000.
- Mobley, C. D., *Light and Water: Radiative Transfer in Natural Waters*, 592 pp., Academic, San Diego, Calif., 1994.
- Morel, A., Diffusion de la lumière par les eaux de mer, Résultats expérimentaux et approche théorique, *AGARD Lect. Ser.*, *61*, 3.1-1–3.1-76, 1973.
- Morel, A., Optical modeling of the upper ocean in relation to its biogenous matter content (case I waters), *J. Geophys. Res.*, *93*, 10,749–10,768, 1988.
- Morel, A., and Y. H. Ahn, Optics of heterotrophic nanoflagellates and ciliates-A tentative assessment of their scattering role in oceanic waters compared to those of bacterial and algal cells, *J. Mar. Res.*, *49*, 177–202, 1991.
- Morel, A., and B. Gentili, Diffuse reflectance of oceanic waters: Its dependence on sun angle as influenced by the molecular-scattering contribution, *Appl. Optics*, *30*, 4427–4438, 1991.
- Morel, A., and L. Prieur, Analysis of variations in ocean colour, *Limnol. Oceanogr.*, *22*, 709–722, 1977.
- Mueller, J. L., and R. W. Austin, Ocean optics protocols for SeaWiFS validation, Revision 1, *NASA Tech. Memo.*, *104566*, 67 pp., 1995.
- Mueller, J. L., and R. E. Lange, Biooptical provinces of the northeast Pacific Ocean-A provisional analysis, *Limnol. Oceanogr.*, *34*, 1572–1586, 1989.
- Nusch, E. A., Comparison of methods for chlorophyll and phaeopigment determination, *Arch. Hydrobiol. Beih. Ergebn. Limnol.*, *14*, 14–36, 1980.
- O'Reilly, J. E., S. Maritorena, B. G. Mitchell, D. A. Siegel, K. L. Carder, S. A. Garver, M. Kahru, and C. R. McClain, Ocean color chlorophyll algorithms for SeaWiFS, *J. Geophys. Res.*, *103*, 24,937–24,953, 1998.
- O'Reilly, J. E., et al., Ocean color chlorophyll *a* algorithms for SeaWiFS, OC2 and OC4, Version 4, *NASA Tech. Memo.*, *2000-206892*, 9–27, 2000.

- Parsons, T. R., Y. Maita, and C. M. Lalli, *A Manual of Chemical and Biological Methods for Seawater Analysis*, 173 pp., Pergamon, New York, 1984.
- Piechura, J., and W. Walczowski, The Arctic front: Structure and dynamics, *Oceanologia*, *37*, 47–73, 1995.
- Platt, T., and S. Sathyendranath, Oceanic primary production: Estimation by remote sensing at local and regional scales, *Science*, *241*, 1613–1620, 1988.
- Reynolds, R. A., D. Stramski, and B. G. Mitchell, A chlorophyll-dependent semianalytical model derived from field measurements of absorption and backscattering coefficients within the Southern Ocean, *J. Geophys. Res.*, *106*, 7125–7138, 2001.
- Sathyendranath, S., G. Cota, V. Stuart, H. Maass, and T. Platt, Remote sensing of phytoplankton pigments: A comparison of empirical and theoretical approaches, *Int. J. Remote Sens.*, *22*, 249–273, 2001.
- Schötz, F., Pigmentanalytische untersuchungen an *Oenothera*: I. Vorversuche und analyse der blätter und blüten von *Oenothera suaveolens* Desf., Mutante “weissherz”, *Planta*, *58*, 411–434, 1962.
- Stramska, M., D. Stramski, B. G. Mitchell, and C. D. Mobley, An inverse model for in-water optical measurements based on radiative transfer simulations, *Limnol. Oceanogr.*, *45*, 628–641, 2000.
- Stramski, D., and D. A. Kiefer, Light-scattering by microorganisms in the open ocean, *Prog. Oceanogr.*, *28*, 343–383, 1991.
- Tassan, S., and G. M. Ferrari, An alternative approach to absorption measurements of aquatic particles retained on filters, *Limnol. Oceanogr.*, *40*, 1358–1368, 1995.
- Trees, C. C., R. R. Bidigare, D. M. Karl, and L. Van Heukelem, Fluorometric chlorophyll *a*: Sampling, laboratory methods, and data analysis protocols, *NASA Tech. Memo.*, 2000-209966, 162–169, 2000.
- Yan, B., K. Stamnes, M. Toratani, W. Li, and J. J. Stamnes, Evaluation of a reflectance model used in the SeaWiFS ocean color algorithm: Implications for chlorophyll concentration retrievals, *Appl. Opt.*, *41*, 6243–6259, 2002.
- Yentsch, C. S., Measurements of visible light absorption by particulate matter in the ocean, *Limnol. Oceanogr.*, *7*, 207–217, 1962.
-
- R. Hapter, S. Kaczmarek, and J. Stoń, Institute of Oceanology, Polish Academy of Sciences, Powstancow Warszawy 55, 81-712 Sopot, Poland. (hapter@iopan.gda.pl; kaczmar@iopan.gda.pl; aston@iopan.gda.pl)
- M. Stramska, Hancock Institute for Marine Studies, University of Southern California, Los Angeles, CA 90089-0371, USA. (stramska@usc.edu)
- D. Stramski, Scripps Institution of Oceanography, University of California at San Diego, La Jolla, CA 92093-0238, USA. (stramski@mpl.ucsd.edu)